https://doi.org/10.21289/KSIC.2023.26.6.993

Design of a Novel Polishing Tool Mechanism with 3-axis Compliance

Gi-Seong Kim[1], Han Sung Kim[2*]

〈Abstract〉

In this paper, a novel polishing tool mechanism with 3-axis compliance is presented, which consists of 2-axis rotational and 1-axis linear compliances in series. The 2-axis rotational compliance mechanism is made up of four cantilever beams for adjusting rotational stiffness and one flexure universal joint at the center for constraining the z-axis deflection. The 2-axis rotational compliance can mechanically adjust the polishing tool to machined surfaces. The polishing press force can be simply controlled by using a linear spring along the z-axis. The 2-axis rotational and 1-axis linear compliance design is decoupled. The stiffness analysis of the 2-axis compliance mechanism was performed based on link compliance matrix and rigid body transformation. A 3-axis polishing tool was designed by configuring the 2-axis compliance mechanism and one linear spring.

Keywords : Polishing Tool, Compliance, Stiffness, Decoupled, Flexure Universal Joint

1 Dept. of Mechanical Convergence Engineering, Kyungnam University
Email: shark-cat@hanmail.net
2* Corresponding author, Dept. of Mechanical Engineering, Kyungnam University, Professor
Email: hkim@kyungnam.ac.kr

1. Introduction

Polishing refers to as the process of smoothing or giving gloss to the surface of a processed product. It is mainly used for trimming and finishing various products such as metal, plastic, and glass. To ensure accurate and precise work, polishing tasks require skilled workers [1]. Polishing tasks are repetitive and require only a small number of skilled workers due to the high intensity of the work. Additionally, it is difficult for even skilled workers to work for long periods of time [2]. Recently, polishing tasks using robots become important, and research has been conducted to apply a constant force by providing polishing tools with compliance similar to that of workers [3]. In order to increase the precision of polishing, research has been conducted on position/force control of robots based on force sensors [4] and force control considering the rigidity of the robot [5]. In addition, research was also conducted on simultaneous position/force control using AI to create machining paths [6]. In previous studies, the position/force control was performed by using a 6-axis compliance device [7-10].

In this paper, a polishing tool mechanism with 3-axis compliance is presented, which consists of 2-axis rotational and 1-axis linear compliances in series. First, the stiffness of the 2-axis rotational compliance mechanism is derived in an analytical manner. Second, the stiffness matrix becomes diagonal by changing design parameters. Finally, the prototype of the polishing tool with 3-axis compliance is designed by simply adding linear springs to the 2-axis rotational compliance mechanism in series.

2. Stiffness Analysis of a 2-axis Rotational Compliance Mechanism

This chapter presents the stiffness analysis of a 2-axis rotational compliance mechanism. First, the working direction of the polishing tool is defined as shown in Fig. 1. The

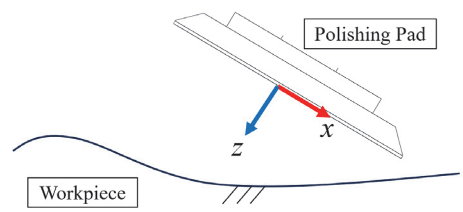

Fig. 1 Definition of polishing tasks

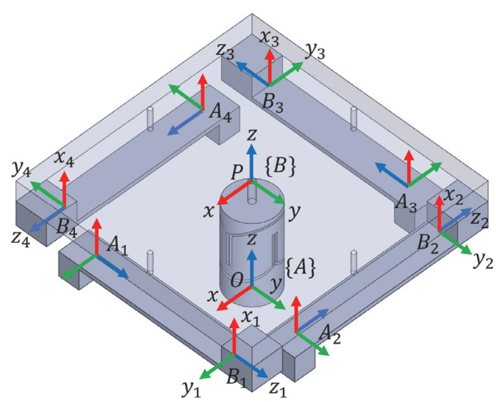

Fig. 2 Conceptual design of a 2-axis rotational compliance mechanism with four cantilever beams and one flexure universal joint

direction along the z-axis is the direction in which the polishing tool applies force to the workpiece, and the directions about the x- and y-axes are the directions of rotational compliance for the polishing tool to be in close contact with the workpiece. The polishing press force is defined as f_z, and the reaction moments are defined as n_x, n_y. The 2-axis rotational compliance mechanism is shown in Fig. 2. Additionally, the frame $\{B_i\}$ is $B_i - x_i y_i z_i$ for $i = 1,2,3,4$. Fig. 3 [11] is modeled as Euler-Bernoulli beams with the frame ki as the origin. The compliance matrix of a cantilever beam can be obtained by Eq. (1).

$$F_{ki} = \begin{bmatrix} \frac{L^3}{3EI_y} & 0 & 0 & 0 & \frac{L^2}{2EI_y} & 0 \\ 0 & \frac{L^3}{3EI_x} & 0 & -\frac{L^2}{2EI_x} & 0 & 0 \\ 0 & 0 & \frac{L}{AE} & 0 & 0 & 0 \\ 0 & -\frac{L^2}{2EI_x} & 0 & \frac{L}{EI_x} & 0 & 0 \\ \frac{L^2}{2EI_y} & 0 & 0 & 0 & \frac{L}{EI_y} & 0 \\ 0 & 0 & 0 & 0 & 0 & \frac{L}{GI_p} \end{bmatrix} \quad (1)$$

where A and L denote link area and length; E and G are the modulus of elasticity and shear modulus; and I_x, I_y and I_p are the area moments of inertia about the x- and y-axes, and the polar area moment of inertia, respectively.

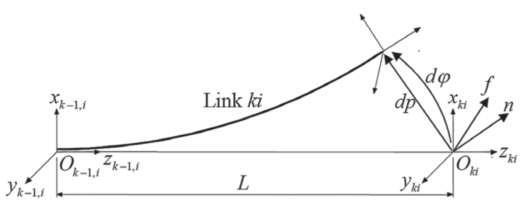

Fig. 3 Elastic model of link ki

The structure of four cantilever beams in Fig. 2 has linear compliance along the z-axis as well as rotational compliance, according to Eq. (1). By employing a flexure universal joint at the center, the linear compliance along the z-axis can be almost eliminated. The resulting structure has only 2-axis rotational compliance about the x- and y-axes.

Quantities specified in a local frame L are combined with others in another reference frame G by introducing 6×6 rigid body transformations.

$$^{G}E_L = \begin{bmatrix} ^{G}R_L & ^{G}\hat{\mathbf{p}}_L\,^{G}R_L \\ 0 & ^{G}R_L \end{bmatrix} \quad (2)$$

where $^{G}R_L$ is the rotation matrix in frame G of frame L, $^{G}\hat{\mathbf{p}}_L$ is the vector in frame G from origin G to origin L expressed as a 3×3 skew-symmetric matrix.

Referring to Fig. 4(a), the compliance matrix $^{Bi}F_{1i}$ for the i^{th} cantilever beam in frame $\{B_i\}$ can be expressed in frame $\{B\}$ by the following transformation.

$$^{B}F_{1i} = {^{B}E_{Bi}}\,{^{Bi}F_{1i}}\,{^{B}E_{Bi}^{T}} \quad \text{for } i = 1,2,3,4 \quad (3)$$

Since the four cantilever beams are connected in parallel to the moving platform, the stiffness matrix by four cantilever beams, $^{B}K_B = {^{B}F_B^{-1}}$ is obtained by

$$ {}^{B}F_{B}^{-1} = \sum_{i=1}^{4} {}^{B}F_{1i}^{-1} \tag{4} $$

The one rotational axis of a flexure universal joint can be modeled as two small cantilever beams as shown in Fig. 4(b). The compliance matrix ${}^{B5j}F_{2j}$ for the j^{th} small beam in frame $\{B_{5j}\}$ can be expressed in frame $\{B\}$ by the following transformation.

$$ {}^{B}F_{2j} = {}^{B}E_{B5j} {}^{B5j}F_{2j} {}^{B}E_{B5j}^{T} \quad \text{for } j = 1,2 \tag{5} $$

Since two small beams are connected in parallel, the compliance matrix of one rotational axis of a flexure universal joint is obtained by

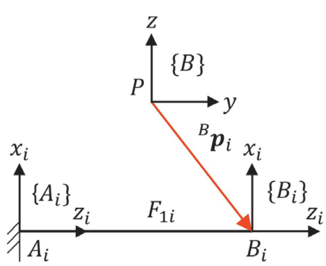

(a) i^{th} cantilever beam

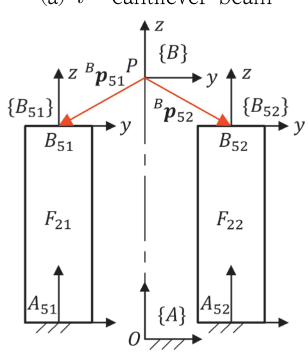

(b) Flexure universal joint

Fig. 4 Frame definitions of a 2-axis rotational compliance mechanism

$$ {}^{B}F_{2}^{-1} = \sum_{j=1}^{2} {}^{B}F_{2j}^{-1} \tag{6} $$

Since the two perpendicular rotational axes of a universal joint are connected in series, the resulting compliance matrix of a flexure universal joint, ${}^{B}F_{U}$ can be obtained by the sum of two compliances.

$$ {}^{B}F_{U} = {}^{B}F_{2} + {}^{B}R_{z} {}^{B}F_{2} {}^{B}R_{z}^{T} \tag{7} $$

where ${}^{B}R_{z}$ is the rotational matrix about the z-axis by 90°.

Therefore, the stiffness matrix of the 2-axis rotational compliance mechanism can be obtained as follows.

$$ {}^{B}K = {}^{B}F_{B}^{-1} + {}^{B}F_{U}^{-1} \tag{8} $$

3. Design of a 3-axis Polishing Tool

In this chapter, a polishing tool with 3-axis compliance was designed based on the stiffness analysis in the previous chapter. The 3-axis compliance can be designed by the 2-axis rotational compliance mechanism and the 1-axis linear compliance with compression springs.

The stiffness matrix ${}^{B}K$ for a 2-axis rotational compliance mechanism is expressed by

$$
{}^{B}K=\begin{bmatrix} k_{11} & 0 & 0 & 0 & k_{15} & 0 \\ 0 & k_{22} & 0 & k_{24} & 0 & 0 \\ 0 & 0 & k_{33} & 0 & 0 & 0 \\ 0 & k_{42} & 0 & k_{44} & k_{45} & 0 \\ k_{51} & 0 & 0 & k_{54} & k_{55} & 0 \\ 0 & 0 & 0 & 0 & 0 & k_{66} \end{bmatrix} \quad (9)
$$

In the case of $p_{ix}=p_{iy}$ of the position vector, ${}^{B}\boldsymbol{p}_i=[p_{ix}, p_{iy}, p_{iz}]^T$ in Fig. 4(a), the stiffness matrix becomes $k_{45}=k_{54}=0$. For numerical calculation, the four cantilever beams (material: SUS304) are selected with 52 mm length, 15 mm width, and 1.5 mm thickness. The overall cantilever beam dimensions are designed considering 100×100mm polishing tool size. Depending on the z coordinate, p_{5jz} of ${}^{B}\boldsymbol{p}_{5j}$ in Fig. 4(b), the off-diagonal elements $k_{15}=k_{51}$ and $k_{24}=k_{42}$ can converge to 0. The z coordinate indicates the center of the universal joint. Therefore, the stiffness matrix become a diagonal matrix when the frame $\{B\}$ is at the center of the flexure universal joint and $p_{ix}=p_{iy}$. The design variables for a diagonal stiffness matrix are $p_{ix}=p_{iy}=50.5\text{mm}$ and $p_{5jz}=7.5\text{mm}$.

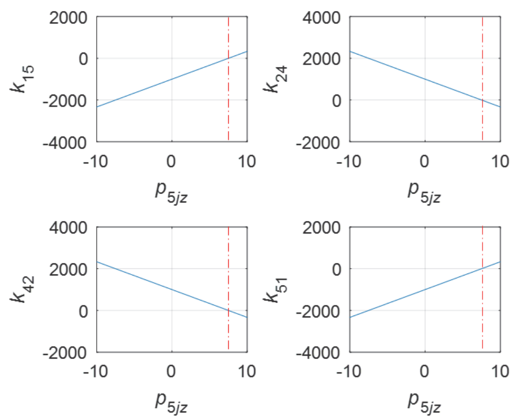

Fig. 5 Off-diagonal elements in the stiffness matrix, ${}^{B}K$ according to p_{5jz}

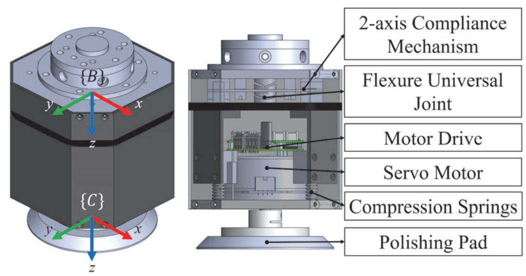

Fig. 6 3D modeling of the 3-axis polishing tool

In Fig. 6, 3D modeling for the 3-axis polishing tool is presented. In addition, it is possible to attach a displacement sensor along the compression springs and to calculate polishing press force by spring constant (k_z). Since the 2-axis rotational compliance mechanism is connected in series with the linear spring, the total stiffness can be obtained by

$$
{}^{B}K_T=diag[k_{11}, k_{22}, k_{33}^{'}, k_{44}, k_{55}, k_{66}] \quad (10)
$$

where $k_{33}^{'-1}=k_{33}^{-1}+k_z^{-1}$. The total compliance matrix $({}^{B}F_T={}^{B}K_T^{-1})$ in frame $\{B\}$ can be obtained by

$$
{}^{B}F_T=diag[f_{11}, f_{22}, f_{33}, f_{44}, f_{55}, f_{66}] \quad (11)
$$

Table 1. Diagonal elements of ${}^{B}F_T$

Total compliance	Unit	Value
f_{11}	mm/N	5.61×10^{-6}
f_{22}		5.61×10^{-6}
f_{33}		3.89×10^{-2}
f_{44}	rad/Nm	1.96×10^{-3}
f_{55}		1.96×10^{-3}
f_{66}		1.16×10^{-6}

The total compliance expressed in frame $\{B\}$ is shown in Table 1. The total compliance matrix of the 3-axis compliance mechanism in frame $\{C\}$ at the polishing tool tip can be expressed by

$$ {}^{C}F_{T} = {}^{C}E_{B}\ {}^{B}F_{T}\ {}^{C}E_{B}^{T} \tag{12} $$

The total compliance matrix in frame $\{C\}$ has off-diagonal elements. Off-diagonal elements are much smaller than diagonal ones. In Table 2, only diagonal elements of the total compliance matrix at the tool tip are presented. Comparing Table 2 with Table 1, f_{11} and f_{22} are increased due to the distance from $\{B\}$ to $\{C\}$ and the rotational compliances of f_{44} and f_{55}. The proposed polishing tool has finite 2-axis rotational compliance values of f_{44} and f_{55} and 1-axis linear compliance value of f_{33}. The other diagonal compliance elements have smaller values as expected.

Table 2. Diagonal elements of ${}^{C}F_{T}$

Total compliance	Unit	Value
f_{11}	mm/N	7.07×10^{-3}
f_{22}		7.07×10^{-3}
f_{33}		3.89×10^{-2}
f_{44}	rad/Nm	1.96×10^{-3}
f_{55}		1.96×10^{-3}
f_{66}		1.16×10^{-7}

Table 3. Compliance analysis accuracy

Rotational compliance	f_{44} [rad/Nm]	f_{55} [rad/Nm]
Theory	1.96×10^{-4}	1.96×10^{-4}
FEM	2.06×10^{-4}	2.06×10^{-4}
Error	4.85%	4.85%

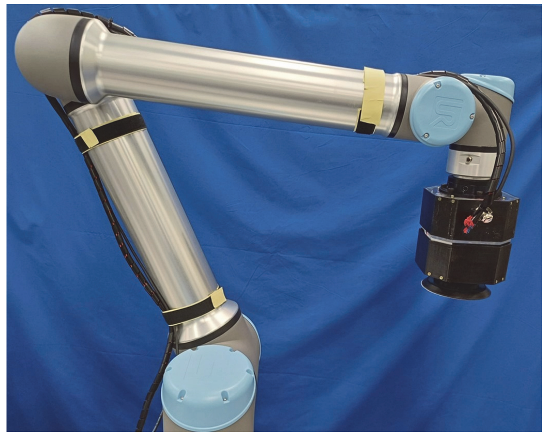

Fig. 7. Prototype of the 3-axis polishing tool

Table 3 shows the error between the analytical calculation and finite element method (FEM) analysis for f_{44} and f_{55}, and the error is less than 5%.

Based on the design method, a prototype of the 3-axis polishing tool is developed and attached at the UR10e robot as shown in Fig. 7.

4. Conclusions

In this paper, a novel 3-axis compliance mechanism is proposed for a robotic polishing tool. It is noted that the 2-axis rotational and 1-axis linear compliance design is decoupled. The analytical stiffness analysis for the 2-axis rotational compliance mechanism is performed and verified through FEM analysis. The prototype of the polishing tool with 3-axis compliance is developed. In future research, precision polishing control based on the force/moment measurements will be conducted.

Acknowledgements

This research was supported by "Regional innovation Strategy (RIS)" through the National Research Foundation of Korea(NRF) funded by the Ministry of Education(MOE) (2021RIS-003)

References

[1] Nobuaki E. et al, “Application of Model Predictive Control to Polishing Robot for Pushing Operation,” ICCAS, pp. 518-522, (2022).
[2] Yuxin D. et al, “A Review of Robot Grinding and Polishing Force Control Mode,” IEEE ICMA, pp. 1416-1418, (2022).
[3] Zhiyun H. et al, “Design of a Novel Force Controlled Polishing Device Based on a Coupled Active-Passive Compliant Mechanism,” IEEE ICMA, pp. 986-991, (2023).
[4] Chuntao Z. et al, “Design of an Industrial Robot Polishing Control System,” IEEE ICMRA, pp. 14-18, (2022).
[5] Hafidz M. D. and Hsien-I L. “Improvement of Force Performance in Robotic Polishing Tasks with Position Compensation,” ICSSE, pp. 412-417, (2023).
[6] Srinivasan L. et al, “An adaptive framework for robotic polishing based on impedance control,” IJAMT, pp. 401-417, (2021).
[7] Kim H. S. “Design of a 6-axis Compliance Device with F/T sensing for Position/Force Control,” KSIC, vol. 21, no. 2, pp. 63-70, (2018).
[8] Kim H. S. “Kinestatic Control using Six-axis Parallel-type Compliant Device,” KSMTE, vol. 23, no. 5, pp. 421-427, (2014).
[9] Park S. B. and Kim H. S. “Position/force Control using 6-axis Compliance Device for Chemical Coupler Assembly,” KSIC, vol. 25, no. 5, pp. 909-915, (2022).
[10] Kim G. S., Jeong S. H., Kim H. S. “Study on the Stability of Force Control using a 6-axis Compliance Device with F/T Sensing,” KSIC, vol. 26, no. 1, pp. 211-215, (2023).
[11] Kim H. S. and Lipkin H. “Stiffness of Parallel Manipulators With Serially Connected Legs,” Transactions or the ASME, vol. 6, pp. 1-9, (2014).

(Manuscript received November 16, 2023;
revised November 24, 2023; accepted December 06, 2023)